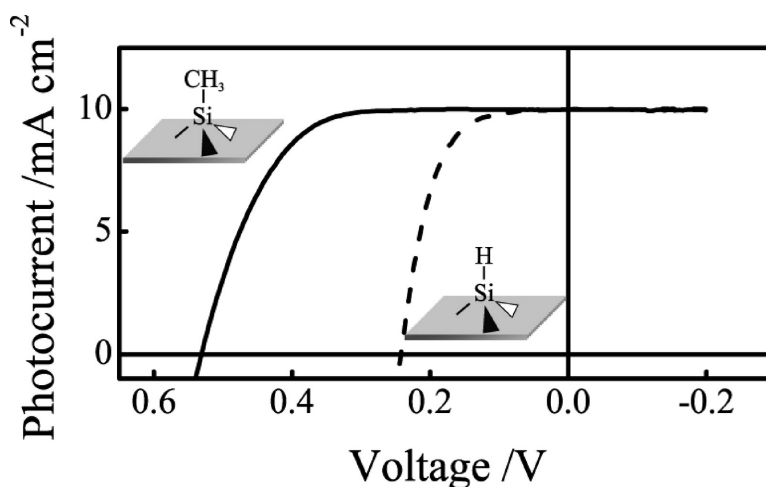


Near-Ideal Photodiodes from Sintered Gold Nanoparticle Films on Methyl-Terminated Si(111) Surfaces

Stephen Maldonado, David Knapp, and Nathan S. Lewis

J. Am. Chem. Soc., **2008**, 130 (11), 3300-3301 • DOI: 10.1021/ja800603v

Downloaded from <http://pubs.acs.org> on February 8, 2009



More About This Article

Additional resources and features associated with this article are available within the HTML version:

- Supporting Information
- Access to high resolution figures
- Links to articles and content related to this article
- Copyright permission to reproduce figures and/or text from this article

[View the Full Text HTML](#)

Near-Ideal Photodiodes from Sintered Gold Nanoparticle Films on Methyl-Terminated Si(111) Surfaces

Stephen Maldonado, David Knapp, and Nathan S. Lewis*

Beckman Institute and Kavli Nanoscience Institute, 210 Noyes Laboratory, 127-72, Division of Chemistry and Chemical Engineering, California Institute of Technology, Pasadena, California 91125

Received January 24, 2008; E-mail: nslewis@caltech.edu

Control over the electrical properties of semiconductor/metal junctions is of importance in electronics, chemical sensing, and energy conversion applications. For materials such as Si, the barrier height of semiconductor/metal Schottky barriers is relatively insensitive to the work function of the metal, due to the formation of metal silicides and/or the presence of other interfacial processes that occur during junction formation. One means of circumventing this problem is to modify the semiconductor surface with moieties that prevent the interfacial reaction from occurring, thereby recovering control over the electrical properties of such Schottky junctions.

Modification of Si(111) surfaces with CH₃- groups has been shown to protect the surface chemically while introducing an interfacial dipole, changing an ohmic contact to a highly rectifying junction for “soft” Hg contacts made on n-Si(111) surfaces.¹ However, for reactive metals such as Au or Cu, even fully CH₃-terminated Si(111) surfaces are not sufficiently stable against metal silicide formation during conventional thermal evaporation, resulting in sub-optimal, Fermi-level pinned junctions.² To prepare such Si/metal junctions without sacrificing chemical control over the interfacial electronic properties, alternative, softer metal deposition strategies are necessary.

Recently, soft metal deposition strategies such as indirect e-beam metal evaporation^{3,4} or lift-off-float-on (LOFO) junction formation⁵ have been developed. InP/Au and TiO₂/metal nanoparticle (NP) junctions have also been prepared from insulating layers of encapsulated, charged Au NPs or discrete metal/semiconductor nanocomposites, respectively.^{6–9} We report herein the use of butanethiol-capped, 2–4 nm Au NPs as useful soft precursors for unpinned, high quality macroscale Schottky junctions using CH₃-terminated Si. In this approach, the NP layers are used as precursors to semitransparent, conductive, and macroscale metal top contacts. Such cast metal NP films, when deposited onto CH₃-terminated n-Si(111) surfaces and sintered to remove the encapsulant alkylthiol ligand,¹⁰ result in Schottky junctions that are free of deleterious interfacial reactivity between Au and Si, and produce unpinned Si/Au contacts without the need for either expensive metal deposition instrumentation and/or a buffer oxide layer.

The reported Si Schottky junctions employed nondegenerately doped n-Si(111) substrates that had been either H-terminated² (aged ≤30 min) or CH₃-terminated¹¹ (aged 1–30 days) prior to use. The preparation of the tested devices is detailed in the Supporting Information. Figure 1 shows representative current density (*J*) versus voltage (*V*) data for the tested devices. n-Si/Au junctions formed from evaporated Au films on freshly H-terminated Si(111) yielded open-circuit voltages, *V*_{oc}, of 0.25–0.3 V at light intensities sufficient to produce short-circuit photocurrent densities, *J*_{sc}, of 10 mA cm⁻². Such devices are well-known to be limited by thermionic emission of electrons over the 0.7–0.8 eV barrier at the n-Si/Au interface.¹² Similarly prepared devices employing CH₃-terminated

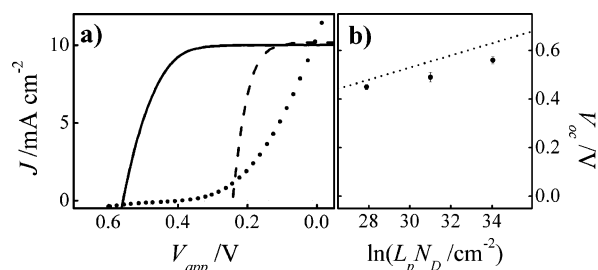


Figure 1. (a) Current density versus voltage responses for n-Si/Au devices using (---) H-terminated n-Si(111) with an evaporated Au film, (····) H-terminated n-Si(111) with a sintered Au NP film, and (—) CH₃-terminated n-Si(111) with a sintered Au nanoparticle film. The illumination intensities were adjusted to generate short circuit current densities of 10 mA cm⁻². (b) Measured *V*_{oc} values versus ln(*L*_p*N*_D) for n-Si/Au devices made with CH₃-terminated n-Si(111) and sintered Au NP films. The dotted line represents the bulk-recombination-limited *V*_{oc}.

n-Si(111) exhibited noticeably higher values of *V*_{oc} (Table 1) but were still limited by interfacial majority-carrier charge-transfer processes. Devices prepared from sintered Au NP films on H-terminated n-Si(111) showed, on average, higher *V*_{oc} values than analogous devices with evaporated Au. However, such junctions exhibited poor fill factors (*FF*). In contrast, n-Si/Au devices made from deposition of sintered Au NP films on CH₃-terminated Si(111) exhibited much higher *V*_{oc} values, while maintaining good fill factors (Figure 1). The photoresponses of such junctions also showed substantial stability, with excellent *J*-*V* responses persisting for several weeks (Supporting Information).

A quantitative analysis of the *V*_{oc} values for the Au NP precursor-based devices on CH₃-Si(111) indicates that their energy conversion performance is limited by the properties of the bulk Si. For photosensitive junctions with n-type semiconductor absorber layers, the maximum obtainable *V*_{oc} is determined by bulk diffusion/recombination processes within the semiconductor, according to the Shockley diode equation¹² (eq 1):

$$V_{oc} = \frac{k_B T}{q} \ln\left(\frac{J}{J_0}\right) = \frac{k_B T}{q} \ln\left(\frac{J_{sc} L_p N_D}{q D_p n_i^2}\right) \quad (1)$$

Here, *J*₀ and *J*_{sc} are the dark saturation current and short circuit photocurrent densities, *L*_p is the minority-carrier (hole) diffusion length, *N*_D is the bulk majority-carrier dopant density, *D*_p is the minority-carrier diffusion coefficient, *k*_B is Boltzmann’s constant, *T* is the temperature, *n*_i is the intrinsic carrier concentration in the semiconductor, and *q* is the charge on an electron. Figure 1b shows the measured *V*_{oc} values for devices made with CH₃-terminated n-Si(111) and sintered Au NP films, as a function of the bulk properties of Si. The experimentally measured *V*_{oc} values were close to the calculated bulk-recombination-limited *V*_{oc} values, and linearly increased with larger values of ln(*L*_p*N*_D), in agreement with eq 1.

Table 1. Open-Circuit Voltages and Fill Factors of n-Si/Au Devices^a

N_b (cm^{-3}) ^b	L_p (μm) ^c	device type ^d	no. ^e	V_{oc}/V	FF
$(5.9 \pm 0.1) \times 10^{13}$	220	CH ₃ -Si/AuNP	7	0.45 ± 0.01	0.59 ± 0.03
$(1.1 \pm 0.1) \times 10^{15}$	274	H-Si/Au evap	6	0.31 ± 0.01	0.56 ± 0.02
		CH ₃ -Si/AuNP	12	0.49 ± 0.02	0.59 ± 0.07
		CH ₃ -Si/Au evap	6	0.38 ± 0.02	0.65 ± 0.01
		H-Si/AuNP	12	0.37 ± 0.12	0.16 ± 0.05
$(3.1 \pm 0.1) \times 10^{16}$	194	H-Si/Au evap	6	0.29 ± 0.01	0.63 ± 0.02
		CH ₃ -Si/AuNP	6	0.56 ± 0.02	0.56 ± 0.09
		H-Si/Au evap	4	0.24 ± 0.01	0.61 ± 0.02

^a Illuminated with a tungsten-halogen lamp so $J_{sc} = 10 \text{ mA cm}^{-2}$.
^b Measured by 4-point probe methods. ^c Assuming rapid recombination at the back ohmic contact, $L_p \approx$ half the wafer thickness. ^d AuNP = sintered Au nanoparticle film. ^e Number of tested devices.

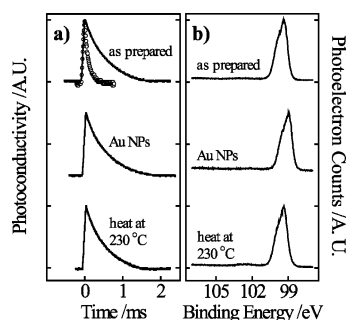


Figure 2. (a) Time-resolved photoconductivity decays of H-terminated (O) and CH₃-terminated (—) Si(111) in air after various treatments. Top: photoconductivity transients of H-terminated Si(111) after 10 min in air versus CH₃-terminated Si(111) after 2 days in air. Middle: CH₃-terminated Si(111) after soaking for 30 min in a CH₂Cl₂ suspension of Au NP. Bottom: CH₃-terminated Si(111) soaked in the Au NP suspension and then heated in vacuum at 230 °C for 30 min. (b) X-ray photoelectron spectra of CH₃-terminated Si(111) after treatments as in (a).

This behavior is in contrast to the behavior of junctions between H-terminated n-Si(111) and evaporated Au films (Table 1), which were insensitive to the bulk Si properties and thus dominated by junction-based recombination.

The difference between the J - V behavior for sintered Au NP film devices made on H-terminated and CH₃-terminated Si(111) surfaces, respectively, can be understood in terms of the relative stability and electronic properties of the different surfaces under ambient conditions. Figure 2 displays time-resolved photoconductivity decay and X-ray photoemission spectroscopy (XPS) data for the surfaces of interest. The time-resolved photoconductivity decays of float-zone-grown Si(111) following a pulsed light ($\lambda = 830$ or 905 nm , Supporting Information) excitation yield the rate of photoexcited charge-carrier recombination at the surface, which in turn yields a value for the surface recombination velocity, S .¹¹ As shown in Figure 2a, H-terminated Si(111) surfaces exhibited large values of S ($500 \pm 140 \text{ cm s}^{-1}$) after only 10 min in air. In contrast, CH₃-terminated Si(111) surfaces exposed to ambient conditions for over 48 h still exhibited relatively low S values, $S = 45 \pm 7 \text{ cm s}^{-1}$. Subsequent immersion of CH₃-Si(111) surfaces for 30 min in CH₂Cl₂ suspensions of Au NP, in addition to heating at 230 °C for 30 min, did not significantly decrease S (Table S1). Consistently, H-terminated Si(111) substrates exhibited significant oxide signatures in their Si 2p XP spectra after soaking in suspensions of Au

NP in CH₂Cl₂, commensurate with a surface oxide thickness of 2.2 \AA . In contrast, as shown in Figure 2b, high-resolution Si 2p XP spectra of CH₃-terminated Si(111) substrates showed relatively little oxidation after each of the same process steps described in Figure 2a. From the adjusted ratios of the integrated signal intensities, the oxide thickness observed after each process step was $<1.2 \text{ \AA}$, i.e., <0.35 monolayers. Thus, coating of the CH₃-terminated Si(111) surface with Au NPs either before or after sintering did not lead to appreciable surface oxide growth, in contrast with the well-documented activity of Au for catalyzing the oxidation of H-terminated Si surfaces.¹³

The electronic quality of CH₃-terminated Si(111) surfaces is thus remarkably durable even after prolonged storage and processing. The combination of CH₃-terminated Si(111) and butanethiol-capped Au NP precursors allows for the formation of high quality Si/Au junctions without extensive formation of an interfacial Au silicide layer or production of a substantial, thick surface oxide, as demonstrated by the observed V_{oc} values. Unlike formal metal–insulator–semiconductor (MIS) device structures, which utilize oxide films that are several monolayers in thickness ($d \geq 8 \text{ \AA}$), the devices reported here represent MIS-type architectures in which the interfacial layer is composed of alkyl groups covalently bonded to the Si surface atoms. In addition to the CH₃- groups on the Si(111) surfaces, residual butanethiol groups still attached to the coalesced Au film may aid in buffering chemical interactions between the Au and Si atoms. These n-Si/Au junctions therefore contain a completely “organic” interfacial layer that supports large ratios of hole to electron injection currents.

Acknowledgment. We gratefully acknowledge the National Science Foundation, grant No. CHE-0604894, for support of this work. S.M. also acknowledges financial support from the Ford Foundation, through the National Academies of Sciences.

Supporting Information Available: Experimental details for the synthesis and characterization of Au NPs, device fabrication, film morphology, J - V data collection, photoconductivity decay measurements, and XP spectra collection/analysis. This material is available free of charge via the Internet at <http://pubs.acs.org>.

References

- Maldonado, S.; Plass, K. E.; Knapp, D.; Lewis, N. S. *J. Phys. Chem. C* **2007**, *111*, 17690–17699.
- Hunger, R.; Fritsche, R.; Jäckel, B.; Webb, L. J.; Jaegermann, W.; Lewis, N. S. *Surf. Sci.* **2007**, *601*, 2896–2907.
- Haick, H.; Niitsoo, O.; Ghabboun, J.; Cahen, D. *J. Phys. Chem. C* **2007**, *111*, 2318–2329.
- Haick, H.; Ambrico, M.; Ghabboun, J.; Ligonzo, T.; Cahen, D. *Phys. Chem. Chem. Phys.* **2004**, *6*, 4538–4541.
- Moons, E.; Bruening, M.; Shanzer, A.; Beier, J.; Cahen, D. *Synth. Met.* **1996**, *76*, 245–248.
- Boettcher, S. W.; Strandwitz, N. C.; Schierhorn, M.; Lock, N.; Lonergan, M. C.; Stucky, G. D. *Nat. Mater.* **2007**, *6*, 592–596.
- Cozzoli, P. D.; Fanizza, E.; Comparelli, R.; Curri, M. L.; Agostiano, A.; Laub, D. *J. Phys. Chem. B* **2004**, *108*, 9623–9630.
- Wood, A.; Giersig, M.; Mulvaney, P. *J. Phys. Chem. B* **2001**, *105*, 8810–8815.
- Subramanian, V.; Wolf, E. E.; Kamat, P. V. *J. Am. Chem. Soc.* **2004**, *126*, 4943–4950.
- Wu, Y. L.; Li, Y. N.; Liu, P.; Gardner, S.; Ong, B. S. *Chem. Mater.* **2006**, *18*, 4627–4632.
- Royea, W. J.; Juang, A.; Lewis, N. S. *Appl. Phys. Lett.* **2000**, *77*, 1988–1990.
- Kumar, A.; Rosenblum, M. D.; Gilmore, D. L.; Tufts, B. J.; Rosenbluth, M. L.; Lewis, N. S. *Appl. Phys. Lett.* **1990**, *56*, 1919–1921.
- Shabtai, K.; Cohen, S. R.; Cohen, H.; Rubinstein, I. *J. Phys. Chem. B* **2003**, *107*, 5540–5546.

JA800603V